Challenges for MR-based Attenuation Correction in PET Imaging of the Head

A. J. van der Kouwe[1,2], C. Catana[1,2], T. Benner[1,2], C. J. Michel[3], M. Hamm[4], S. Nielles-Vallespin[5], S. Kannengiesser[5], M. Fenchel[5], B. R. Rosen[1,2], and A. G. Sorensen[1,2]

[1]Athinoula A. Martinos Center for Biomedical Imaging, Massachusetts General Hospital, Charlestown, MA, United States, [2]Department of Radiology, Harvard Medical School, Brookline, MA, United States, [3]Siemens Medical Solutions USA Inc., Knoxville, TN, United States, [4]Siemens Medical Solutions USA Inc., Charlestown, MA, United States, [5]Siemens Healthcare, Erlangen, Germany

INTRODUCTION

Systems that simultaneously acquire MRI and PET have been developed for small animal [1,2] and human [3] imaging. An MR-compatible prototype PET insert (Siemens BrainPET) was installed in a 3T TIM Trio (Siemens, Erlangen, Germany). Due to limited space in the scanner bore, the insert has no transmission source. The system is also not combined with a CT scanner. Therefore, information traditionally acquired for PET attenuation correction (AC) is not available. Correct AC is critical for meaningful analysis of PET data [4], especially in quantitative studies. We report on progress using MR for PET AC. Using MR for this purpose has the advantage of reducing the subject's radiation exposure and the total examination time, and eliminates co-registration errors between the emission data and AC map. However, MR signal intensity does not relate directly to tissue linear attenuation. In particular, MR sequences provide good soft tissue contrast but are insensitive to bone. Therefore bone and air, with the highest and lowest linear attenuation coefficients for photons, are indistinguishable using traditional MR techniques. We report on the use of ultrashort echo time (UTE) sequences for bone segmentation and the need to include the RF coil in the AC map.

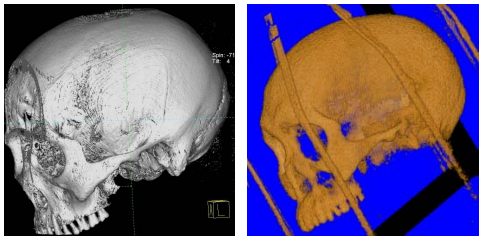

Fig. 1: CT scan (200 μm isotropic) (left) and MR UTE image (approx. 1.5 mm isotropic) (right) of human skull. MR image shows location of 8-channel RF coil elements (bars) relative to skull.

MATERIALS AND METHODS

UTE Sequences and Bone Segmentation: UTE sequences are used to image tissues with short T2* relaxation times [5], such as bone. We imaged a human skull with a dual-echo radially encoded gradient echo sequence (TE 70 μs/4 ms, TR 6 ms, FA 10˚, 32768 projections, T_{acq} 8 x 3:17 (26:16) min:s, 8 channel BrainPET coil, T_{dwell} 1.7 μs) on a 3T TIM Trio system and with a Siemens volume CT scanner (120 kV/50 mA, T_{acq} 20 s). Bone is identified by thresholding the difference between early and late echo UTE images. Typical short UTE acquisitions result in larger voxels, and when tissues such as fat are present, UTE voxels may contain multiple competing components that drown out the bone signal and may need to be fitted separately to the acquired data.

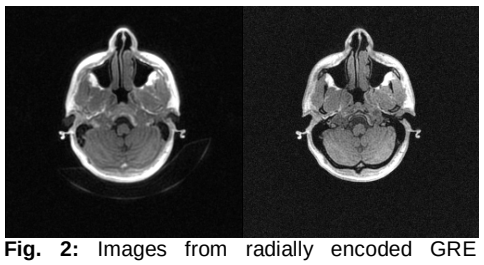

Fig. 2: Images from radially encoded GRE sequence with TE 70 μs (left) and 2.4 ms (right).

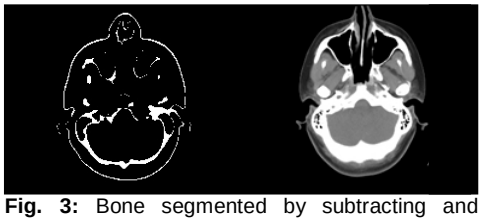

Fig. 3: Bone segmented by subtracting and thresholding the two images of Figure 2 (left). Similar slice of CT image acquired for a different subject (right).

RF Coil Attenuation: Another factor that has to be considered in implementing accurate AC in a combined MR-PET scanner is the attenuation of the RF coil located between the patient and the PET detectors. The precise position and attenuation properties of the coil must be known. The position of the RF coil is usually fixed, and the attenuation coefficients of its components can be determined from a CT scan. Such a scan for the BrainPET birdcage coil is shown in Figure 4. We studied the effect of the coil attenuation on the image quality by simulating a 20 cm water phantom filled with activity. Uniform emission (e.g. 10 counts/voxel) was assumed. The μ-map was obtained by assuming a constant 0.096 cm^{-1} linear attenuation coefficient across the phantom, combined with the converted HU obtained from the CT images of the coil. The emission volume was forward projected to obtain the emission sinogram. Similarly, the attenuation sinograms have been obtained by forward projecting the μ-map of the cylinder not including and including the coil. The emission sinogram was "attenuated" using the "correct" attenuation sinogram to obtain the "trues" sinogram. The images were reconstructed from the "trues", attenuation and normalization sinograms.

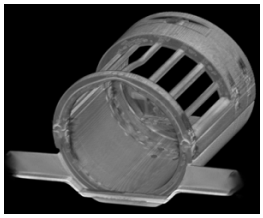

Fig. 4: CT of birdcage coil.

RESULTS AND DISCUSSIONS

UTE Sequences and Bone Segmentation: Figure 1 shows 3D reconstructions of the skull imaged with CT and MR UTE. These images could be tightly registered, with negligible distortions on the scale of conventional CT used for AC purposes. Figure 2 shows UTE acquisitions at TE 70 μs and 2.4 ms. Bone is visible at the first echo time and not the second. Figure 3 shows the thresholded difference between the UTE echoes together with a CT scan showing good correspondence with bone in a different subject. Note the poor axial resolution of conventional clinical CT (2.5/5 mm). A thin fat layer at the tissue-air interface was misclassified as bone. The need to include bone in AC for PET head scans is established in an accompanying abstract.

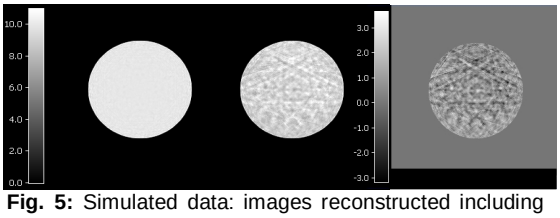

Fig. 5: Simulated data: images reconstructed including (left) and not including (middle) AC for the RF coil, with the difference image (right).

RF Coil Attenuation: Reconstructed images without/with AC for the birdcage coil, and the difference, are shown in Figure 5. Degradation in image uniformity is evident. This effect may be amplified in this particular scanner by the gaps between the detectors in the axial/transaxial directions. The data demonstrate that coil attenuation cannot be ignored if quantitative data is needed. Figure 1 demonstrates that MR UTE data can be used to measure the coil position and shape (for flexible coils), since the coil elements are clearly visible in the image.

REFERENCES: [1] Catana C et al, PNAS, 2008; 105(10): 3705-10; [2] Judenhofer MS et al, Nature Medicine, 2008; 14(4):459-465; [3] Schlemmer HP et al, Radiology, 2008; 248(3):1028-35; [4] Zaidi H et al, E JNM&MI, 2004; 31(1): 52-63; [5] Tyler DJ et al. J Magn Reson Imaging 2007; 25:279-289.